

Horizontal Connections for Precast Concrete Shear Walls Subjected to Cyclic Deformations Part 2: Prestressed Connections

Khaled A. Soudki, Ph.D.

Adjunct Assistant Professor and
NSERC Post-Doctoral Fellow
Department of Civil Engineering
Queen's University
Kingston, Ontario, Canada



This paper represents the second part of a multiphase experimental program undertaken at the University of Manitoba to study the cyclic behavior of prestressed connections for precast concrete shear walls. The first part of the study dealt with the behavior of mild steel connections. In this paper, the results of testing five full-scale prestressed connections subjected to reversed cyclic combined flexure and shear loads are presented. The connections were also subjected to axial stresses normal to the connection to simulate gravity loads. The paper discusses the influence of cyclic vs. monotonic loading, use of prestressed strands vs. prestressed bars and the effect of fully unbonded prestressed bars on the behavior of the connections. Based on the test results, design recommendations for the prestressed connection in seismic zones are presented. A simple analytical procedure is developed to predict the envelope of cyclic response and a numerical design example is included to illustrate the design procedure.



Sami H. Rizkalla Ph.D., P.Eng.

Professor
Department of Civil and
Geological Engineering
University of Manitoba
Winnipeg, Manitoba, Canada

Robert W. Daikiw, P.Eng.

Vice President and
General Manager
Lafarge Construction Materials
A Division of Lafarge Canada Inc.
Winnipeg, Manitoba, Canada



The use of prestressed connections for precast concrete shear wall panel systems is not permitted in active seismic zones by most design codes in North America.^{1,2} This is mainly due to the lack of knowledge of how this type of system performs under seismic loading conditions.

In order for prestressed connections to gain acceptance in seismic regions, their cyclic behavior must be examined to determine their energy dissipation and ductility capabilities. As a part of a multiphase experimental study undertaken at the University of Manitoba, prestressed connection specimens were tested to investigate the behavior of horizontal connections for precast concrete shear wall panels subjected to reversed cyclic combined flexure and shear loads.³

This paper, Part 2 of the study, reports on the cyclic behavior of prestressed connections. The behavior of mild steel connections under similar loading conditions is presented in a companion paper as Part 1.⁴

RESEARCH SIGNIFICANCE

The behavior of prestressed connections for precast concrete shear wall systems is presented. The connections were subjected to reversed cyclic combined flexure and shear loads in addition to constant stress normal to the connection.

The results are used to determine strength, stiffness, ductility, energy dissipation and failure modes of these types of connections. A numerical example is given to illustrate a proposed procedure to predict the envelope of the cyclic response of prestressed connections. Design recommendations for prestressed connections for precast shear walls in seismic zones are presented.

EXPERIMENTAL PROGRAM

Connection Configuration

Three different prestressed horizontal connection configurations are presented in this paper. The overall geometry of the connections was identical

and used two prestressing continuity reinforcements at 900 mm (35.4 in.) on center, as shown in Fig. 1. The three configurations are as follows:

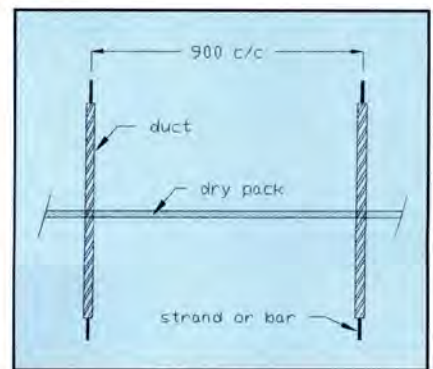
PTS, Post-tensioning strand — This connection was post-tensioned using two 1/2 in. (12.7 mm) diameter 7-wire strands. The drypack was allowed to cure for seven days prior to post-tensioning. The strands were tensioned to 60 percent of their tensile strength to produce a stress of 1.2 MPa (0.175 ksi) normal to the connection. The strands were placed in galvanized steel ducts cast in the panels. After post-tensioning, the ducts were filled with an expansive grout. The grout used was a mixture of high early portland cement, water and non-shrink admixture (1:0.42:0.0086 by part).

PTB, Post-tensioning bar — This connection was post-tensioned using two 5/8 in. (15.8 mm) diameter threaded prestressing Dywidag bars. Seven days after drypacking, the bars were stressed to produce an average stress normal to the connection of 1.2 MPa (0.175 ksi), similar to Connection PTS. The bars were placed inside galvanized steel ducts and after post-tensioning, the ducts were filled with the same expansive grout as used in Connection PTS.

PTBU, Post-tensioning bar unbonded — This connection was identical to Connection PTB, with the exception that the post-tensioned bars were fully unbonded in the top and bottom panels. The bars were placed inside ungrouted plastic ducts.

Test Specimen

Five full-scale prestressed specimens were tested in this experimental program under the effect of combined flexural and shear loading conditions. The connections were also subjected to an axial stress normal to the con-



(a) Schematic



(b) Photographic

Fig. 1. Connection configuration.

nection of 2 MPa (0.29 ksi) to simulate gravity loading conditions.

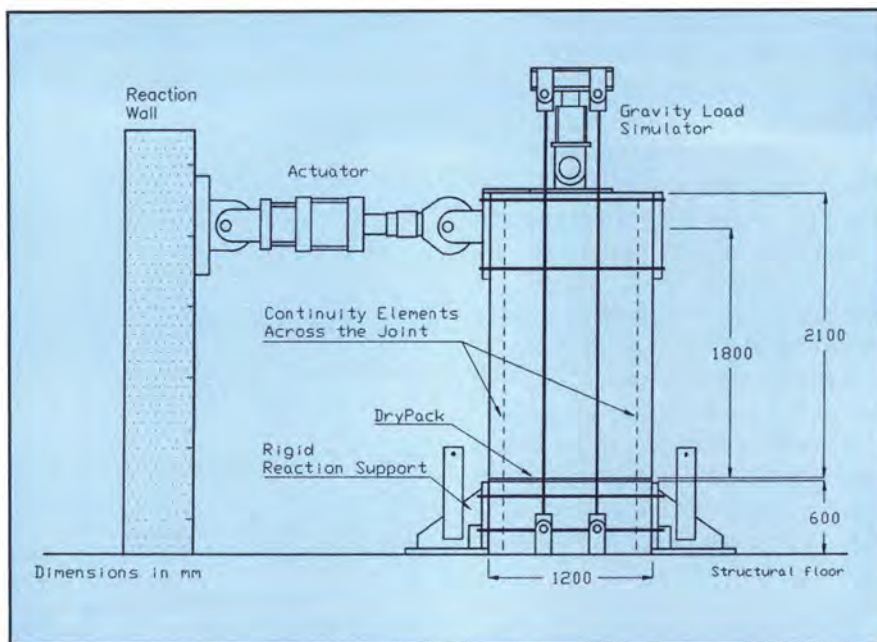
Three specimens were tested under reversed cyclic flexure and shear while the other two specimens were tested under monotonic flexure and shear loading. Table 1 summarizes the experimental program.

The overall connection geometry of the test specimen, material properties, and test setup are identical to the specimens tested in the first phase and reported in the companion paper.⁴ The test setup is shown in Fig. 2.

The test started by load control increments up to yield of the prestressed reinforcement. According to ASTM standards,⁵ the yield strain of prestressed strands is 1 percent while that of prestressed bars is 0.7 percent. After yielding, the loading proceeded in displacement controlled incremental

Table 1. Various connection configurations used in test program.

Connection type	Specimen description	Test method
PTS-S	Post-tensioned strand, bonded	Monotonic
PTB-S	Post-tensioned Dywidag bar, bonded	Monotonic
PTS	Post-tensioned strand, bonded	Cyclic
PTB	Post-tensioned Dywidag bar, bonded	Cyclic
PTBU	Post-tensioned Dywidag bar, unbonded	Cyclic



(a) Schematic



(b) Photographic

Fig. 2. Test setup.

Table 2. Summary of test results for prestressed specimens.

Specimen	Maximum strength (kN-m)	Yield displacement Δ_y (mm)	Ductility μ_Δ	Drift Δ_u/H (percent)	Stiffness, K (kN/mm)		Slip/displacement S_u/Δ_u (percent)
					K_y	K_u/K_y (percent)	
PTS-S	414	4.0	7	1.56	65	—	5.8
PTB-S	423	4.0	11	2.44	66	—	15.6
PTS	432	4.0	6	1.33	44	16	10.8
PTB	402	4.0	6	1.33	47.5	15	12.5
PTBU	362	4.0	14	3.11	39	7	15.2

Note: 1 kip = 4.448 kN; 1 in. = 25.4 mm.

multiples of the yield displacement up to failure. The load history is identical to the first phase of the experimental program as shown in Fig. 4 of the companion paper.⁴

TEST RESULTS

The load-displacement hysteresis loops for the three prestressed specimens subjected to reversed cyclic loading conditions are given in Figs. 3(a) through 3(c). Load-displacement behavior for the two specimens subjected to monotonic loading is shown in Fig. 3(d).

In general, the response was similar to the behavior of the mild steel specimens reported in the companion paper;⁴ however, the effect of prestressing was made obvious by the narrower hysteresis loops and smaller

plastic deformation in comparison to the mild steel specimens subjected to the same loading conditions.

The hysteresis loops of the unbonded bar connection, shown in Fig. 3(c), were narrower and more pinched in comparison to the loops of the bonded bars and strand connections, shown in Figs. 3(a) and 3(b), respectively. All prestressed specimens showed stable hysteretic behavior and were able to maintain the maximum resistance after significant cycling to large deformations well beyond equivalent yield strength of the reinforcements. The behavior under cyclic loading could be characterized in general in three limit states:

I: Linear elastic stage (less than $1\Delta_y$): prior to yielding of reinforcement without any visible damage.

II: Nonlinear ductile stage ($1\Delta_y$ to

$6\Delta_y$): post-yield behavior with nearly stable hysteresis and minor damage without significant joint deterioration.

III: Failure stage (greater than $6\Delta_y$, except for Connection PTBU): significant reduction in load carrying capacity under large deformation. This stage is characterized by severe deterioration of drypack and rupture of bars or strands.

A summary of the measured results for the different configurations tested is given in Table 2. Behavior of the connection can be categorized in the following sequence.

Rocking Behavior

All prestressed connection configurations had very similar rocking characteristics with rigid-body-type motion of the top panel relative to the

bottom panel at the connection region with linear rotation-displacement relationships. This behavior is mainly due to the inherently low stiffness characteristics of the drypack in comparison to that of the concrete panels.

The two bonded reinforcement connections, PTB and PTS, had nearly identical rotational capacities. The unbonded bar connection, PTBU, achieved a higher rotational capacity in comparison to the bonded connection due to debonding of the prestressing bar.

Reduction of Connection Thickness

At high ductility ratios, permanent reduction in the thickness of the connection, caused by crushing and spalling of the drypack along the connection length, was observed for all prestressed specimens subjected to cyclic loading. In this study, the ductility ratio is defined as the ratio of the total displacement, Δ , to displacement at yield, Δ_y .

At a ductility ratio of 6, the thickness reduction was 17 and 13 percent for Connections PTB and PTBU, respectively, and only 3 percent for Connection PTS. As a result of debonding, Connection PTBU survived to a ductility ratio of 14 at which the thickness reduction was 55 percent from the initial thickness of the drypack.

No measurable thickness reduction was noted for the two connections, PTB-S and PTS-S, tested under monotonic loading due to the absence of the reversed grinding effect caused by cyclic loading conditions.

Slip Behavior

All configurations of the prestressed connections subjected to cyclic load experienced minor initial slip response. The slip was also symmetrical and fully recoverable at zero displacement during the initial cycles. At large displacement increments, the slip deformations were irrecoverable, as evidenced by the measured permanent residual slip at zero displacement.

The slip was permanently shifted towards the pull direction for Connections PTB and PTBU due to local

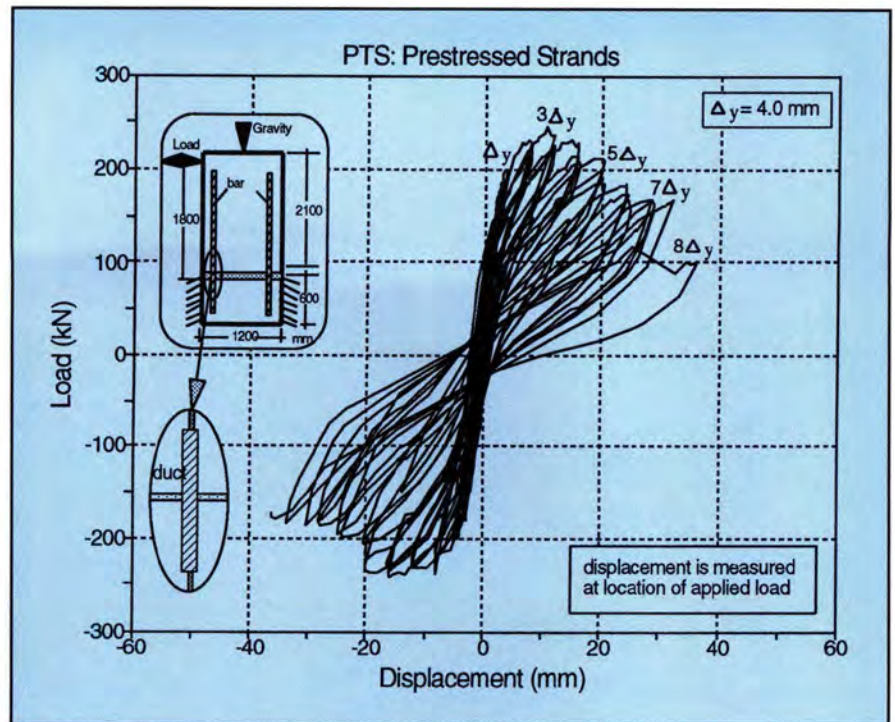


Fig. 3(a). Hysteresis loops behavior for Connection PTS.

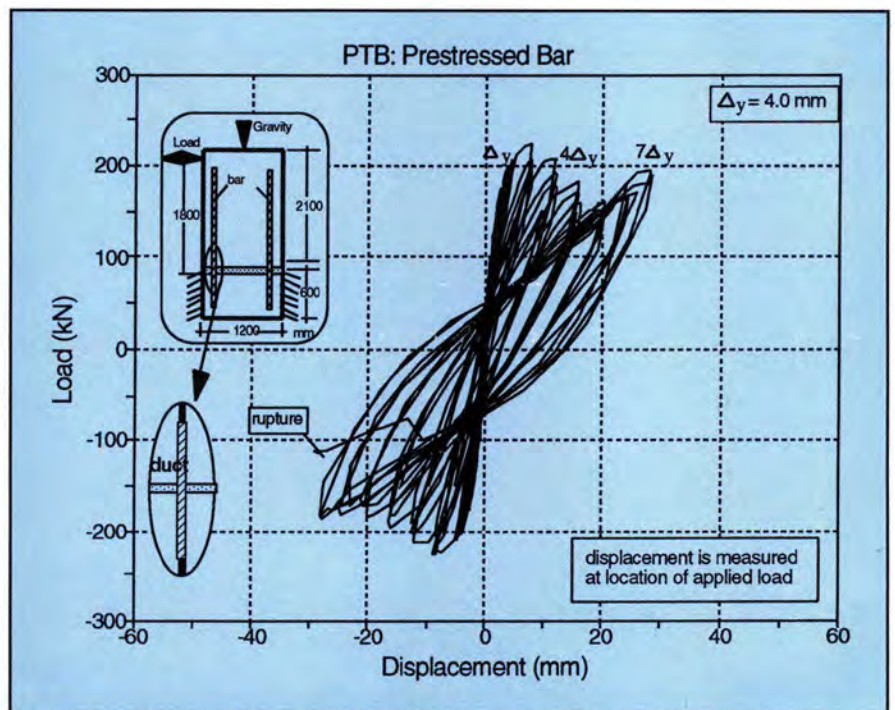


Fig. 3(b). Hysteresis loops behavior for Connection PTB.

shear deformation of the bar at the connection region. This behavior occurred at ductility levels of 4 and 7 for Connections PTB and PTBU, respectively. The slip hysteresis loops were somewhat wide for the bonded connections, PTB and PTS, in comparison to rather narrow loops for the unbonded connection, PTBU.

The maximum slip to the total displacement ratio vs. ductility ratio for the three prestressed connections subjected to cyclic load is compared in Fig. 4. At a ductility ratio of 6, the unbonded connection, PTBU, experienced the lowest slip-to-displacement ratio of 6 percent in comparison to the bonded strands and bar connec-

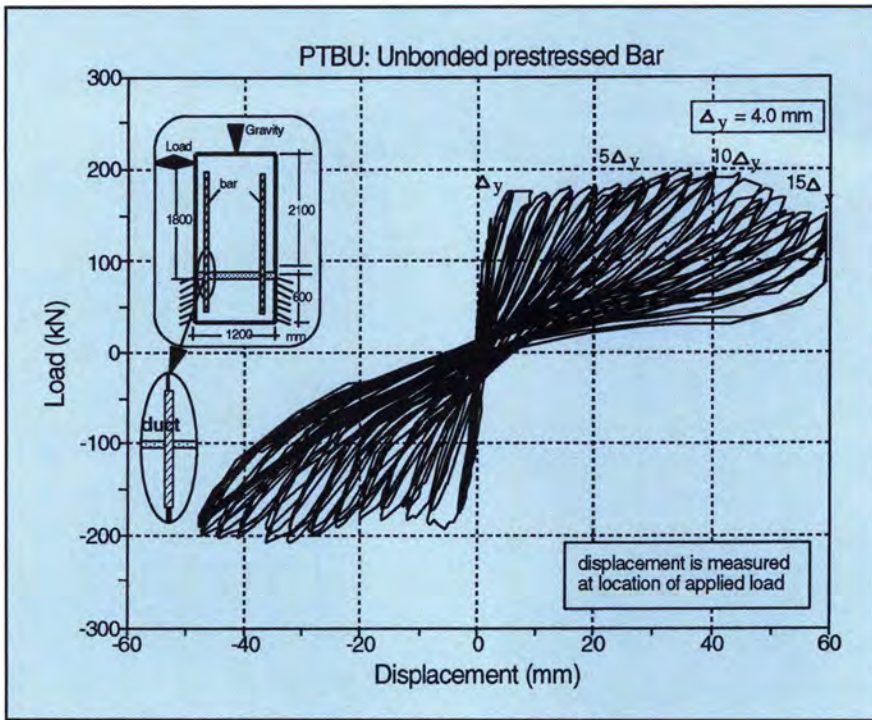


Fig. 3(c). Hysteresis loops behavior for Connection PTBU.

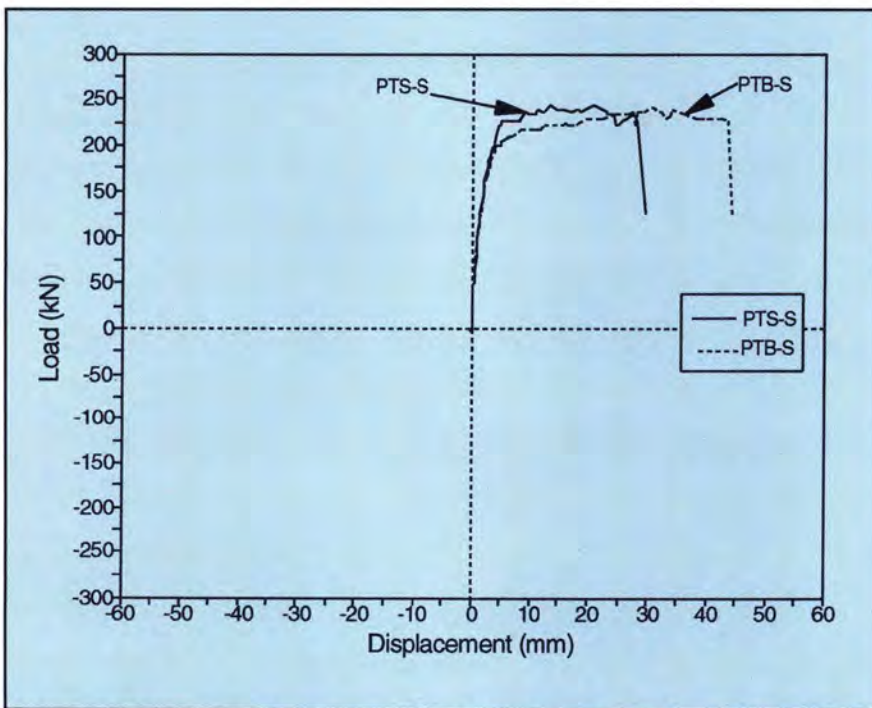


Fig. 3(d). Behavior of Specimens PTS-S and PTB-S subjected to monotonic load.

tions, PTS and PTB, where the ratios were 11 and 12 percent, respectively. This behavior could be attributed to the observed severe degradation of the bonded connection that may have resulted in a significant loss in the prestress in comparison to the unbonded connection, PTBU. The slip-to-displacement ratio was only 14

percent at a ductility ratio of 14 achieved by Connection PTBU.

The slip-to-displacement ratio for Connection PTB-S (with bars) tested under monotonic loads increased from 4 percent at a ductility ratio of 1 to 17 percent at a ductility ratio of 11. Slip of Connection PTS-S (with strands) tested under monotonic loads was

limited to 6 percent of the total deformation throughout the test duration. The slip-to-displacement ratios at ultimate for all connections are compared in Table 2.

Failure Modes

The observed damage at failure varied among the tested prestressed connections, as shown in Fig. 5.

The damage was minor for Connections PTS-S and PTB-S tested under monotonic loading conditions. Crushing of the drypack was concentrated at the extreme end region of the connection; the bulk of the drypack in the compression zone was still intact while the drypack at the outer edges was spalled off. Failure was due to rupture of the strand in Connection PTS at a ductility ratio of 7, and by rupture of the bar in Connection PTB-S at a ductility ratio of 11.

Connection PTS had moderate damage across the connection length at a ductility of 6. The prestressing strand ruptured at the second cycle of $8\Delta_y$, as shown in Fig. 5(a). Severe crushing and spalling of the drypack grout accompanied the rupture of the strand and progressed towards the centerline of the connection. The drypack was ground to a thin layer within the compression zone. Concrete cracking and spalling concentrated at the extreme ends of the connection.

Connection PTB also had moderate damage at a ductility of 6. Failure was by rupture of the prestressing bar at the third cycle of $7\Delta_y$. The drypack at the connection ends was reduced to a very thin layer. Drypack crushing progressed along the full connection length, as shown in Fig. 5(b). Concrete cracking and spalling were mainly in the lower panel and in the form of compression surface cracks.

Connection PTBU had major damage at a ductility of 14. Failure was characterized by severe drypack crushing and spalling over the entire connection length and significant cracking and spalling in the concrete panels at the extreme ends of the connection, as shown in Fig. 5(c). The drypack was literally ground to dust in the connection region. Rupture of the bar did not occur at failure.

Connection Strength

Table 2 compares the strength of the prestressed connections investigated. The connection resistance was determined based on the measured maximum horizontal load located at the top of the upper panel.

The variability in strength among the prestressed connections with bonded reinforcement was within the 7 percent range including the influence of variability of the drypack material. The capacity of the unbonded Connection PTBU was about 90 percent of the strength of the bonded Connection PTB.

The reversed cyclic loading had an apparently insignificant effect on the strength because companion connections tested under monotonic and cyclic loading conditions had identical capacities.

Connection Ductility

All prestressed connections exhibited large deformations without significant loss of strength. Table 2 gives the ductility and drift levels achieved by the different configurations. In this study, the drift is defined as the ratio of the total displacement, Δ , to height of wall panel above the connection region, H .

The connection prestressed with Dywidag bars, PTB-S, tested under monotonic loading exhibited a ductility of 11 and a drift of 2.44 percent. The ductility and drift of the companion connection, PTB, tested under cyclic loading were 6 and 1.33 percent, respectively.

The connection prestressed with strands, PTS-S, tested under monotonic load had a ductility of 7 and a drift of 1.56 percent. The ductility and drift of the companion connection, PTS, under cyclic loading were 6 and 1.33 percent, respectively.

The unbonded connection, PTBU, exhibited the highest ductility of 14 and a drift of 3.11 percent. Therefore, unbonding of the prestressing bars could significantly enhance the ductility of the connection.

Connection Stiffness

The stiffness of the connection is the slope of the peak-to-peak of the load-displacement hysteresis loops at service cycle following each ductility

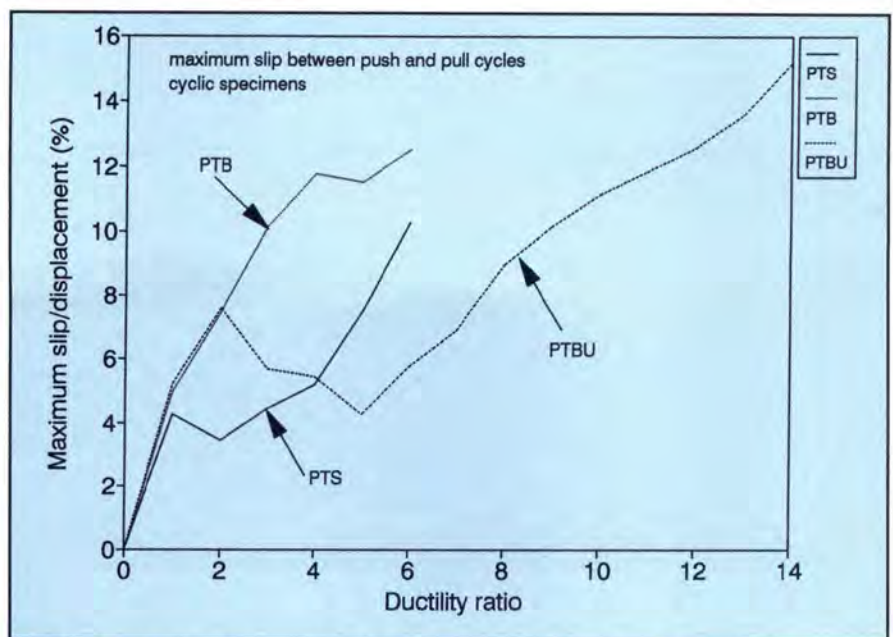


Fig. 4. Comparison of percent slip/displacement for prestressed specimens.



Fig. 5(a). Failure modes for Connection PTS.

increment. The stiffness at first yield, K_y , for the tested connections varied from 47.5 kN/m (3.25 kips per ft) for Connection PTB to 39 kN/m (2.70 kips per ft) for Connection PTBU, as given in Table 2. The 15 percent variability among the stiffness values is due to the use of strands instead of bars and to the debonding effect of the bars used for Connection PTBU.

Fig. 6 presents the degradation of stiffness for the prestressed connections tested under cyclic load in terms of the ratio of measured stiffness to the stiffness at first yield for different ductility levels. Fig. 6 reveals that all tested specimens exhibited a similar

sharp stiffness degradation response.

The residual stiffness at a ductility of 6 is about 15 percent of the stiffness at first yield for the prestressed connections, as shown in Fig. 6 and listed in Table 2. Loss of stiffness is the result of progressive deterioration due to crushing and spalling of the drypack under the effects of cyclic loading conditions.

Energy Dissipation

The energy dissipation per cycle and the cumulative energy dissipation were computed for all prestressed connections subjected to cyclic load. The



Fig. 5(b). Failure modes for Connection PTB.



Fig. 5(c). Failure modes for Connection PTBU.

energy dissipation per cycle is determined as the area enclosed by the load-displacement hysteresis curve. The cumulative energy dissipation is the summation of all the energy dissipated per cycle.

Fig. 7 compares the cumulative energy dissipation for the three prestressed connection configurations subjected to reversed cyclic loading conditions. It is apparent from Fig. 7 that the energy dissipation for all specimens is nonlinear.

Connection PTB, prestressed by bonded bars, provided the highest energy dissipation per cycle while Connection PTBU, prestressed by unbonded bars, exhibited the lowest energy dissipation per cycle up to a

ductility level of 6. However, due to the high ductility level achieved by Connection PTBU, it was possible to gain a significantly higher cumulative energy dissipation before failure at a ductility level of 14.

DISCUSSION OF TEST RESULTS

Effect of Reversed Cyclic Loading

The most significant effect of the cyclic loading on the behavior of the tested prestressed connections is the progressive deterioration of the drypack that represented an additional limit state not observed when the same

connections were tested under monotonic loading conditions.

The deterioration occurred due to a continuous grinding effect and reversal of stresses from compression to tension as a result of the cyclic loading effect. Crushing of the drypack started at the compression zone followed by overall crushing along the entire length of the connection due to grinding action. The degree of deterioration varied and was related to the connection configuration.

The overall strength envelope of the connections subjected to cyclic loading is compared to the behavior of the companion connections tested under monotonic loading in Fig. 8 for the connections prestressed by bars and strands. The behavior indicates that cyclic loading conditions did not affect the maximum strength of the connection and slightly reduced the stiffness at yield.

Degradation was evident at high ductility ratios due to deterioration of drypack. The cyclic loading reduced the deformation capacity considerably from $11\Delta_y$ to $6\Delta_y$ for the connection with prestressed bars and from $7\Delta_y$ to $6\Delta_y$ for the connection prestressed by strands.

Effect of Prestressed Bar vs. Strands

The overall response of Connection PTS, prestressed by strands, was very similar to that of Connection PTB, prestressed by bars, as shown in Fig. 9. Both connections exhibited similar yield displacements and nearly identical stiffness at first yield within the range of 6 percent.

The deformation capacity of the two connections was also similar, as both achieved a ductility of 6. Connection PTS maintained a peak resistance over a slightly larger displacement range while Connection PTB showed some reduction in load prior to maximum deformation capacity.

The damage was more severe for Connection PTB than Connection PTS. Reduction of drypack thickness was 4 percent in Connection PTS vs. 17 percent for Connection PTB. The maximum measured strengths of the two connection types were within a 5

percent range. Connection PTB consistently exhibited 30 percent higher energy dissipation per cycle relative to Connection PTS, as shown in Fig. 7.

In general, both connections with strands and bars exhibit similar characteristics in terms of stiffness, strength, ductility and energy. While connections prestressed by bars have higher energy dissipation, connections prestressed by strands showed more favorable ductile behavior.

Effect of Unbonding

The most significant effect of unbonding the prestressed bars observed is the enhancement of the deformation capacity without significant loss in the strength, as shown in Fig. 9. The deformation capacity for the unbonded connection was 2.33 times that of the bonded connection.

It should be noted that for Connection PTBU, fully unbonded, local yielding of the bars did not occur and, therefore, the measured yield displacement value for the bonded Connection PTB was used as a displacement increment up to failure. As a result of the higher deformation capacity achieved by the unbonded connection, the degree of damage was much more severe in comparison to the bonded connection.

The reduction of the drypack thickness was about 13 percent for the unbonded connection vs. 17 percent for the bonded connection at a ductility ratio of 6. However, the reduction was 55 percent at a ductility ratio of 14 achieved by the unbonded connection.

The hysteresis loops of the unbonded connection were slightly narrower and consequently less energy is dissipated per cycle in comparison to the bonded connection at any given displacement. However, the cumulative energy dissipation was higher for the unbonded connection at failure due to the higher deformation capacity.

Effect of Prestressed vs. Mild Steel Reinforcement

The behavior of mild steel connections and prestressed connections is different due to the differences in the material characteristics used for the continuity reinforcements.

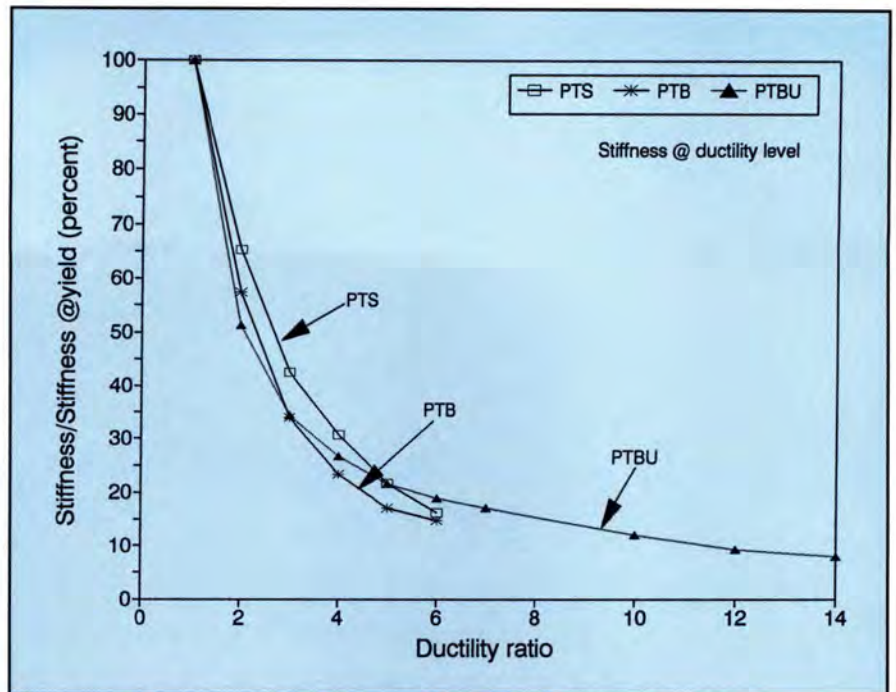


Fig. 6. Stiffness degradation characteristic for prestressed connections.

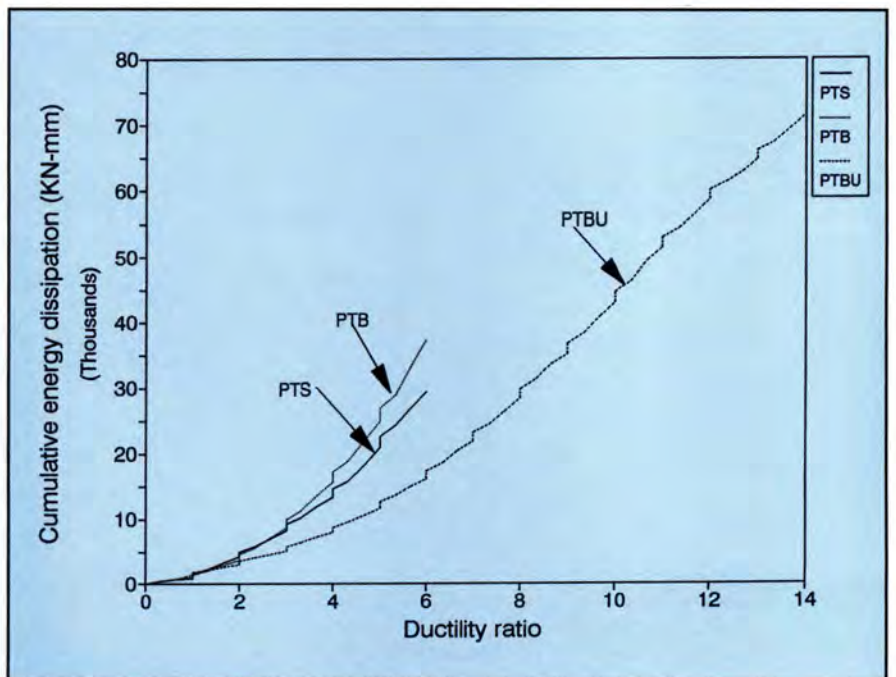


Fig. 7. Cumulative energy dissipation for prestressed specimens.

The hysteresis loops of the prestressed connections were narrower than those in the mild steel connections discussed in the companion paper⁴ and shown in Fig. 10. Therefore, the energy dissipation of the prestressed connection was lower than that for the mild steel connection. This is mainly due to the inherently more ductile material characteristic of the mild steel bars vs. prestressing strands

and bars. At any given ductility level, the energy dissipated by the prestressed connection was about 60 percent that of the mild steel connection.

The deformation capacity expressed in terms of the drift was 1.18 and 1.38 percent for the sleeve and welded mild steel connection configurations, respectively. The drift of the prestressed connections with bars and strands was 1.33 percent.

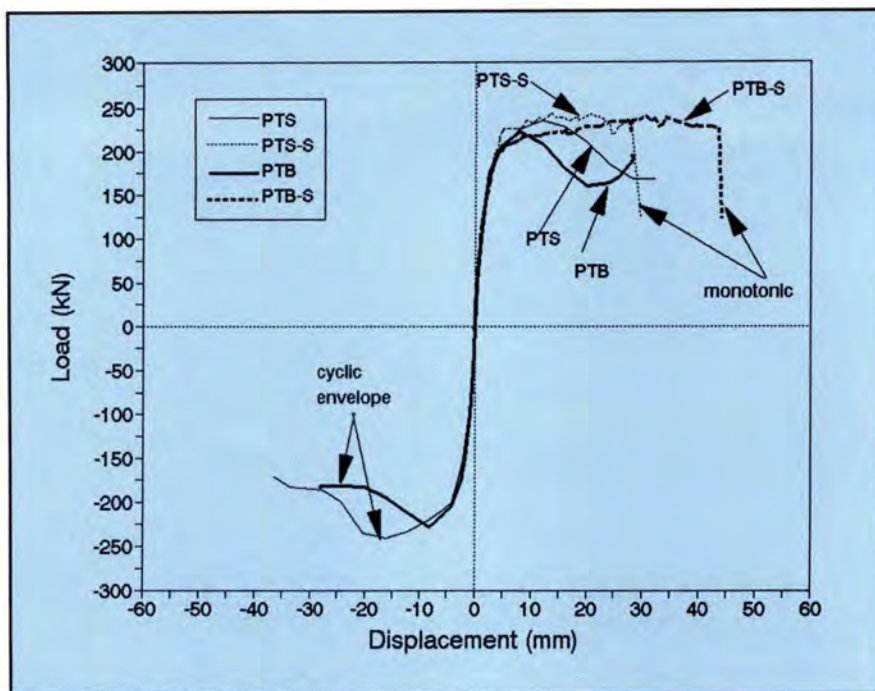


Fig. 8. Effect of cyclic loading on prestressed connections.

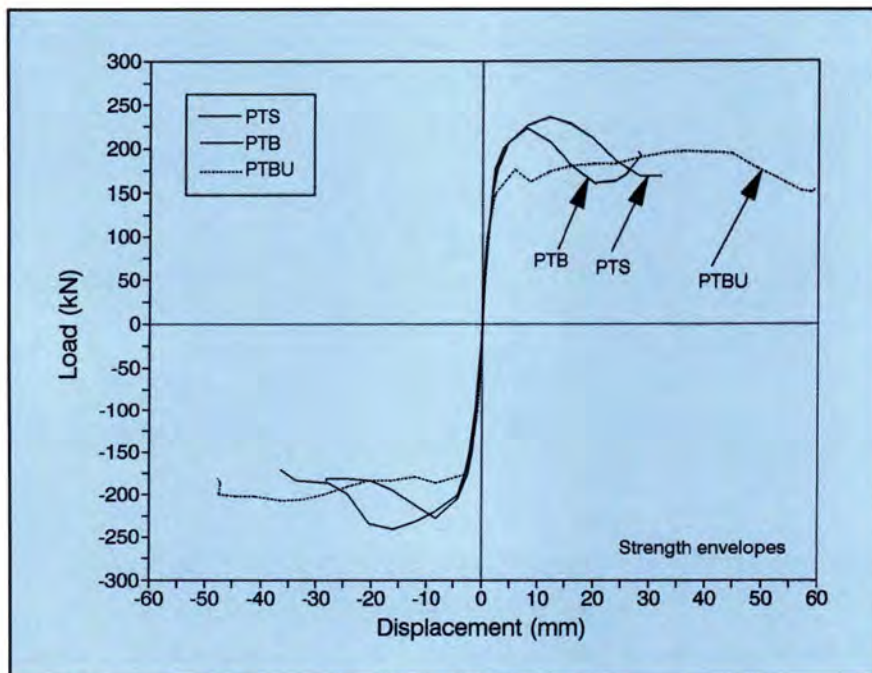


Fig. 9. Comparison of strength envelopes of cyclic response.

Therefore, while prestressed connections possessed lower energy dissipation, they achieved very similar deformation capacities as mild steel connections. Determination of which system to use relies on the designer's judgment in terms of design requirements, economic factors and erection time.

PROPOSED DESIGN PROCEDURE

A simplified design procedure was developed to predict the response of prestressed connections for precast concrete shear walls utilizing characteristics of the materials used in the connection.

Connection Flexural Strength

Flexural strength of the connection can be predicted based on equilibrium and compatibility. The procedure accounts for the reduction in the compression strength of the drypack due to the presence of shear stresses.

The failure criterion of the drypack grout is governed by the interaction of the compressive stresses f_g and shear stresses τ_g at the connection interface. The compression-shear interaction envelope used in this study is based on a parabolic envelope proposed by Llorente⁶ that provided a conservative fit for the measured data by Bresler and Pister,⁷ as shown in Fig. 11.

Three limit states of the connection response should be considered, as shown in Fig. 12. The first state represents yielding of the prestressed reinforcement in tension while the strain in the drypack did not reach its ultimate value, ϵ_{gu} .

The second state, an ultimate state, corresponds to the case when the extreme fiber of the connection reaches the maximum ultimate compression strain of the drypack grout, ϵ_{gu} , and the strain in the prestressing reinforcement is less than ϵ_{pu} .

The third state, an ultimate state, is when the strain in the reinforcement reaches the maximum value, ϵ_{pu} , and results in shifting of the neutral axis away from the edge of the connection due to crushing of the drypack.

Fig. 13 represents a flowchart of the procedure including the above limit states.

Connection Deformation

The total deformation at the top fiber of the upper wall panel, Δ , can be expressed as a combination of slip deformation, Δ_s , and rocking deformation, Δ_r . As discussed in Part 1 of the study,⁴ the slip component of the deformation, Δ_s , represents an unconfined mechanism with no restoring force and, therefore, is not desirable.

It should be mentioned that the measured slip deformation of the tested prestressed connections was varied from 6 to 18 percent of the total deformation, Δ . The flexural deformation, Δ_r , is given in terms of the rotation, θ , and the height of the wall panel above

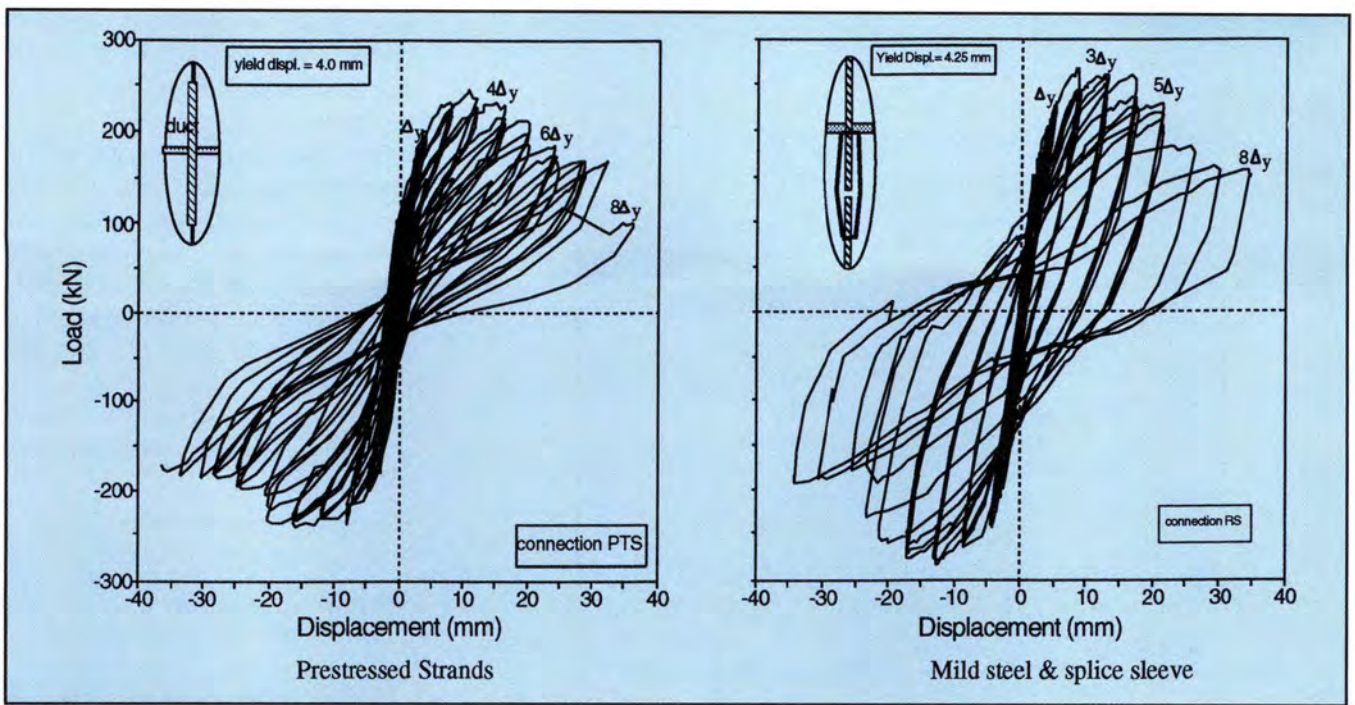


Fig. 10. Effect of prestressed vs. mild steel reinforcement.

the connection, H , as follows:

$$\theta = \frac{\Delta_r}{H} = \frac{\delta_s}{d - c} \quad (1)$$

where

d = distance from reinforcement in tension to extreme edge of connection in compression

c = compression zone depth from extreme edge of the connection in compression

δ_s = extension of prestressed reinforcement

The prestressed reinforcement in the vicinity of the connection develops an elastic region, l_e , and a plastic region, l_p , similar to the one shown in Fig. 14.

The extension of the prestressing reinforcement, δ_s , can be determined by integration of the strain distribution along the tension reinforcement in the upper and lower panel on both sides of the connection region. The extension, δ_s , can be determined as follows:

At yield:

$$\delta_s = 2 \left[\frac{1}{2} (\epsilon_{py} - \epsilon_{pe}) l_e \right] \quad (2)$$

At ultimate:

$$\delta_s = 2 \left[\frac{1}{2} (\epsilon_{py} - \epsilon_{pe}) l_e + (\epsilon_{py} - \epsilon_{pe}) l_p + \frac{1}{3} (\epsilon_{ps} - \epsilon_{py}) l_p \right] \quad (3)$$

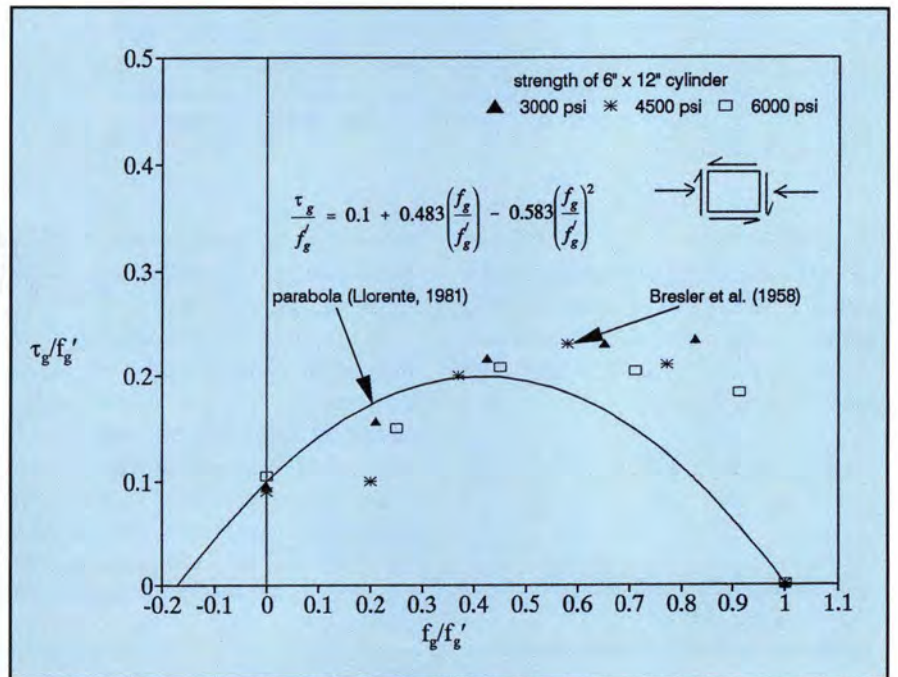


Fig. 11. Compression-shear interaction envelope.

where

ϵ_{pe} = effective prestress strain in reinforcement after losses

ϵ_{py} = equivalent yield strain of prestressed reinforcement

ϵ_{ps} = ultimate strain in tension prestressed reinforcement

It should be mentioned that the compression strain in the drypack due to prestressing is relatively small and, thus, is ignored in the calculations.

The embedment length, l , at any stage depends on the bond strength of the bar, u , bar diameter, d_b , and stress increment in bar, Δf_s , as follows:

$$l = \frac{\Delta f_s d_b}{4u} \quad (4)$$

In the elastic region, the bond strength, u_e , is uniformly distributed and can be expressed using a modified version of an ACI Code equation⁸ as

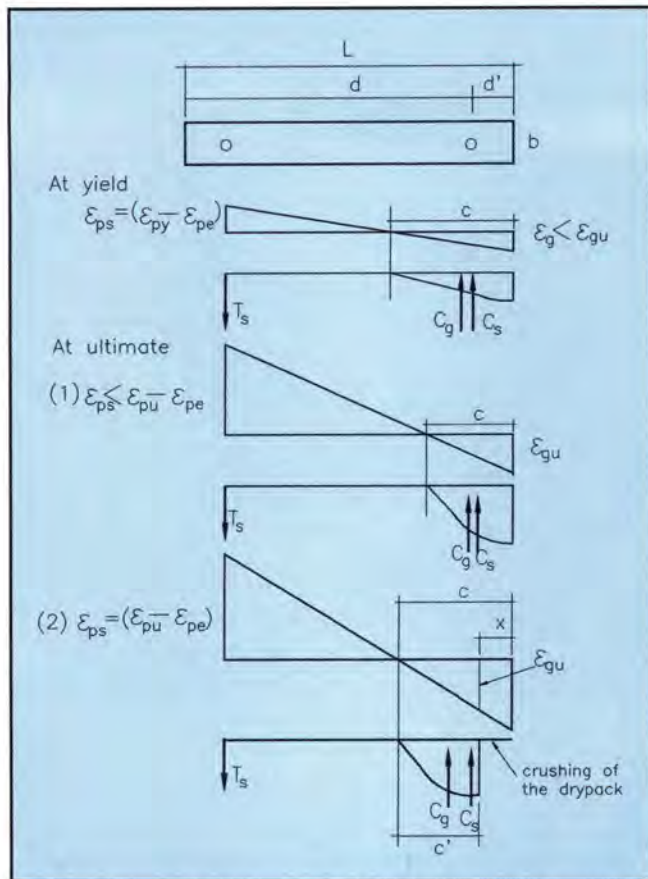


Fig. 12. Connection equilibrium and compatibility at various limit states.

given by French et al.⁹ for mild steel bars. The modified equation includes a multiplier $400/f_{py}$ to account for yield strengths higher than 400 MPa, as recommended by the ACI Code.⁸ The equation is as follows:

$$u = 16 \frac{\sqrt{f'_c}}{d_b} \left(\frac{400}{f_{py}} \right) \text{ (MPa)} \quad (5)$$

where

f'_c = uniaxial compressive strength of concrete, MPa
 f_{py} = yield strength of prestressed reinforcement, MPa

In the plastic region, the bond strength, u_f , can be estimated using a modified version of the expression developed by Pochanart and Harmon¹⁰ for mild steel bars. The modified expression includes the multiplier, $400/f_{py}$, recommended by the ACI Code⁸ to account for yield strengths higher than 400 MPa, as follows:

$$u_f = \left(5.5 - 0.07 \frac{S_b}{H_b} \right) \sqrt{\frac{f'_c}{28}} \left(\frac{400}{f_{py}} \right) \text{ (MPa)} \quad (6)$$

where S_b is the clear spacing of lugs of bar in mm, and H_b is the height of lugs of bar in mm.

In this program, the measured ultimate strain of the prestressed bar, ϵ_{pu} , subjected to reversed cyclic loading condition appears to be limited to 50 percent of the uniaxial tensile strain under monotonic load. This behavior is similar to what was also observed for mild steel bars subjected to cyclic loading as reported by Paulay and Priestley.¹¹

DESIGN EXAMPLE

The connection selected in this example has dimensions similar to the tested connection specimens and is representative of a connection of a precast concrete interior loadbearing shear wall panel at the base of a 10-story building.

The connection geometry is shown in Fig. 15 and is 1200 mm (47.25 in.) long and 152 mm (6 in.) wide with a 20 mm (0.78 in.) drypack thickness. Continuity between the two panels is

provided by two 15.87 mm (⁵/₈ in.) diameter, Grade 1080 MPa (156 ksi), Dywidag bars spaced at 900 mm (35.4 in.) on center.

The distance from tension steel to extreme compression fiber, d , is 1050 mm (41.3 in.) and the distance from compression steel to extreme compression fiber, d' is 150 mm (5.9 in.). The pressure due to the weight of nine stories above the connection is 2 MPa (0.29 ksi).

The characteristics of the various materials used in the connection are as follows:

Concrete: cylinder compressive strength, $f'_c = 45$ MPa (6.52 ksi)

Drypack:

Cube compressive strength,

$f_g'' = 57$ MPa (8.26 ksi)

Cylinder compressive strength,

$f_g' = 0.85 \times f_g'' = 48$ MPa (6.96 ksi)

Ultimate compressive strain,

$\epsilon_{cu} = 0.006$

Prestressed bar:

Area of one bar,

$A_{ps} = 180$ mm² (0.28 in.²)

Yield strength,

$f_{py} = 900$ MPa (130 ksi)

Ultimate tensile strength,

$f_{pu} = 1137$ MPa (165 ksi)

Young's modulus of elasticity,

$E_{ps} = 200,000$ MPa (29,000 ksi)

Yield strain according to ASTM,

$\epsilon_{py} = 0.007$

Monotonic ultimate strain,

$\epsilon_{pu0} = 0.07$

Ultimate strain under reversed

cyclic load ($0.5\epsilon_{pu0}$), $\epsilon_{pu} = 0.035$

Effective prestress after losses,

$f_{pe} = 0.56f_{pu} = 600$ MPa (87 ksi)

Effective prestrain after losses,

$\epsilon_{pe} = 0.003$

Response at yield

The flexural strength at yield can be evaluated by assuming the strain in the continuity bars in tension to be a value equal to $(\epsilon_{py} - \epsilon_{pe})$ and using the equilibrium and compatibility approach to determine the compression zone length. Based on a strain of (0.007 - 0.003), the analysis converges to a compression zone length of 336 mm (13.25 in.) and a compression strain in the drypack grout at the extreme fiber at the edge of the connection of

0.00188, which is less than the ultimate value of 0.006.

The corresponding shear stress at the interface is 3.70 MPa (0.52 ksi) and the compressive strength reduction factor, η , is 0.88, as determined from the failure envelope. The calculated flexural resistance at yield is 330 kN-m (244 kip-ft).

To determine the rotation of the connection using the extension of the reinforcement, the bond stress should be evaluated first using Eq. (5) as:

$$u = 16 \frac{\sqrt{45}}{15.875} \left(\frac{400}{900} \right) = 3.0 \text{ MPa (0.44 ksi)}$$

The elastic length l_e can be determined using Eq. (4) as:

$$l_e = \frac{(900 - 600)(15.875)}{(4)(3.0)} = 397 \text{ mm (15.6 in.)}$$

Therefore, the extension of the bar, δ_s , can be determined by Eq. (2) as:

$$\delta_s = 2 \left[\frac{1}{2} (0.007 - 0.003)(397) \right] = 1.59 \text{ mm (0.063 in.)}$$

The rotation, θ_y , can be evaluated using Eq. (1) as follows:

$$\theta_y = \frac{1.59}{(1050 - 336)} = 0.0022$$

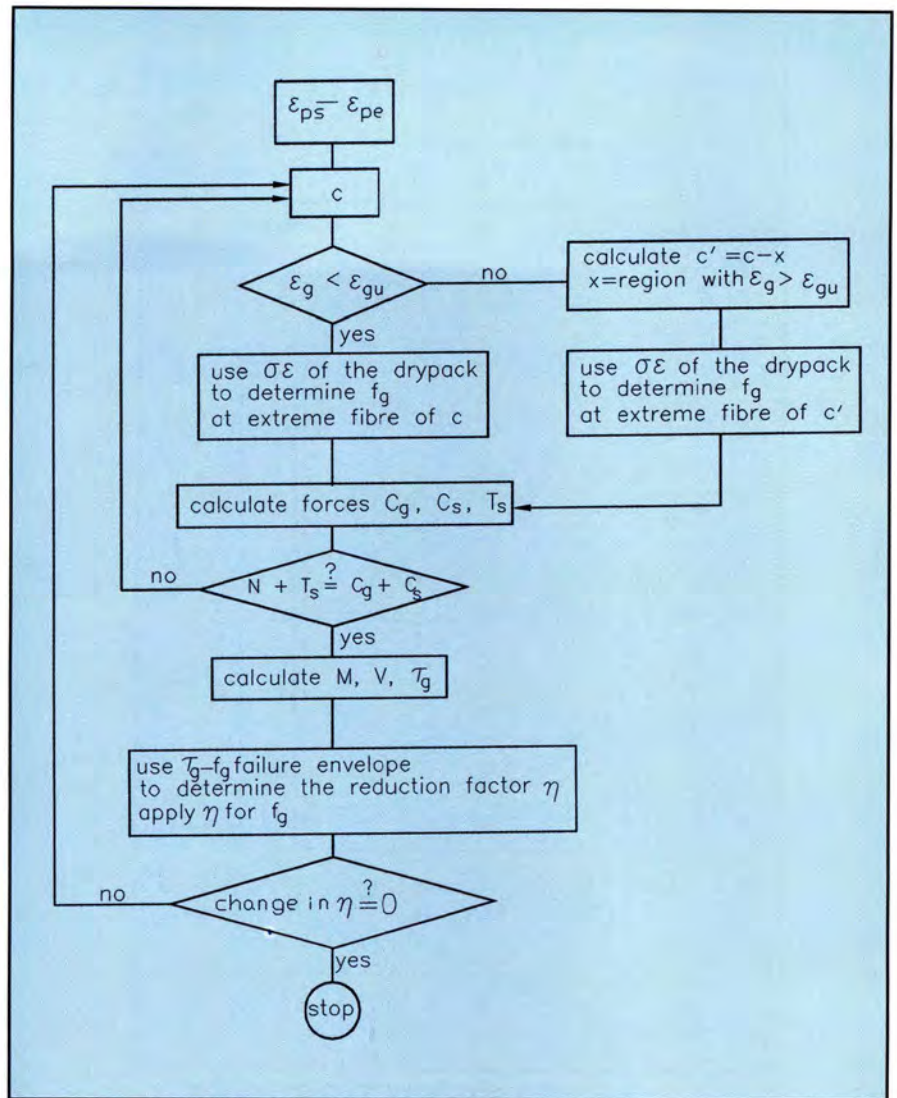


Fig. 13. Flowchart for flexural strength prediction.

Response at Ultimate

Two limit states should be considered at ultimate, as shown in Fig. 12.

Limit State 1 — This limit state corresponds to the case when the extreme fiber of the connection reaches the maximum ultimate compression strain of the drypack grout, ϵ_{gu} , and the strain in the tension reinforcement is less than ϵ_{pu} .

For a strain of 0.006 at the extreme fiber of the connection, the analysis converges to a compression zone length of 190 mm (7.5 in.) and a strain ($\epsilon_{ps} - \epsilon_{pe}$) equal to 0.027 in the tension reinforcement, which represents a total strain of 0.03 in the prestressing bar at this stage. This strain is less than the ultimate strain of 0.035 under reversed cyclic load.

The strength of the connection at

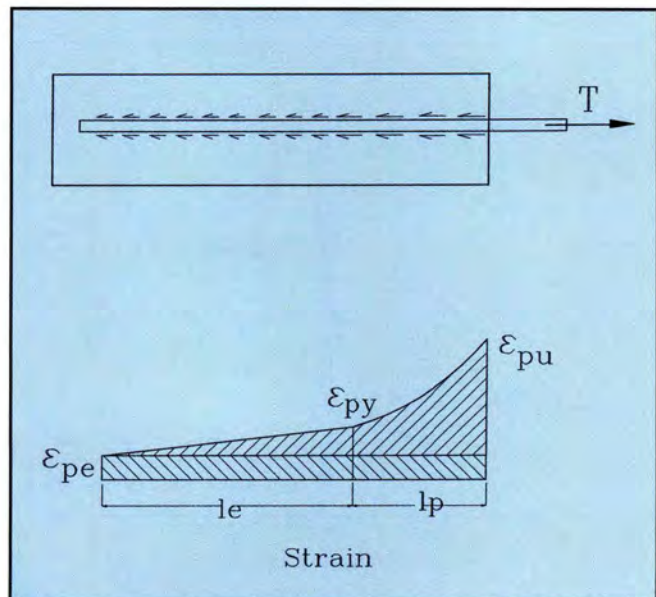


Fig. 14. Strain distribution along prestressed bar in tension.

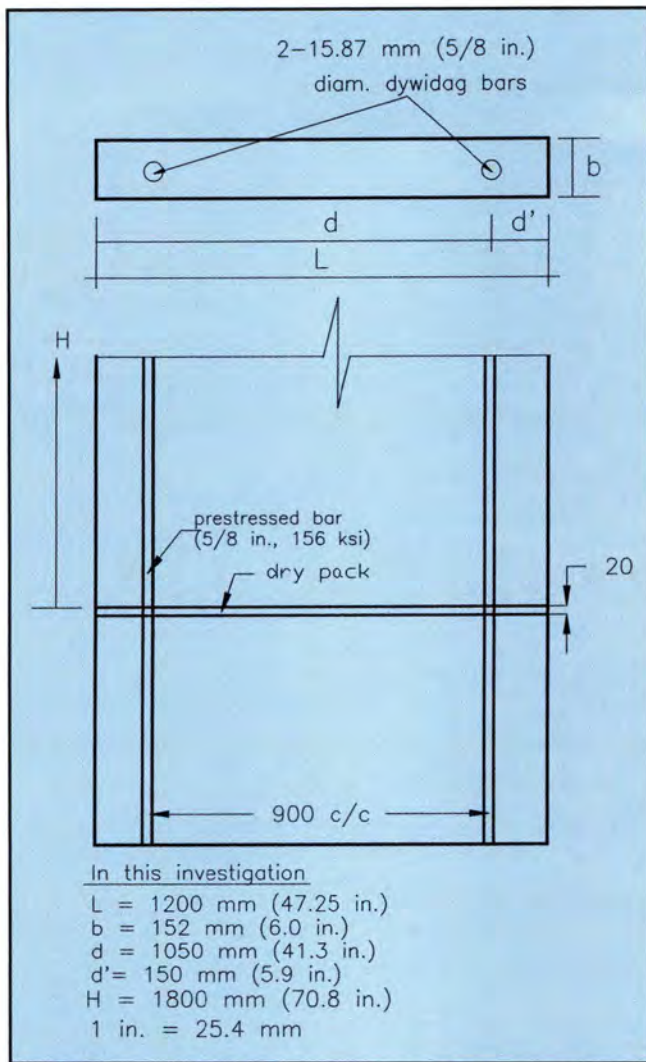


Fig. 15. Connection dimensions used in design example.

this stage is determined from equilibrium and is equal to 384 kN-m (284 kip-ft). The compression strength reduction factor is 0.68, as determined from the failure envelope for shear stress of 7.5 MPa (1.09 ksi).

To determine the rotation at the connection, the frictional bond strength in the plastic region is determined using Eq. (6) as:

$$u_f = \left(5.5 - 0.07 \frac{4}{1} \right) \sqrt{\frac{45}{28} \left(\frac{400}{900} \right)}$$

$$= 3 \text{ MPa (0.43 ksi)}$$

The plastic zone l_p can be determined using Eq. (4) as:

$$l_p = \frac{(1015 - 900)(15.875)}{(4)(3.0)}$$

$$= 152 \text{ mm (6 in.)}$$

Extension of the bar, δ_s , is found from Eq. (3) as:

$$\delta_s = 2 \left[\frac{1}{2} (0.007 - 0.003)(397) + (0.007 - 0.003)(152) + \frac{1}{3} (0.03 - 0.007)(152) \right]$$

$$= 5.14 \text{ mm (0.20 in.)}$$

The rotation at ultimate limit state 1, θ_u , is evaluated using Eq. (1) as follows:

$$\theta_{u1} = \frac{5.14}{(1050 - 190)} = 0.0059$$

Limit State 2 — This state occurs when the strain in the reinforcement reaches the maximum value, ϵ_{pu} , and the extreme fiber of the connection is greater than ϵ_{gu} , which results in shifting of the neutral axis away from the edge of the connection due to crushing of the drypack.

Based on an ultimate strain, $\epsilon_{pu} - \epsilon_{pe}$, of 0.0032, the analysis converges to a compression zone depth, c , of 300 mm (11.82 in.) within which the drypack strain exceeds the ultimate along a length of 160 mm (6.3 in.) and the compression stresses are distributed along a length, c' , of 140 mm (5.51 in.) from the neutral axis.

The drypack strain at the extreme fiber of the connection is 0.0128, i.e., greater than 0.006. The reduction of the grout compressive strength, η , is

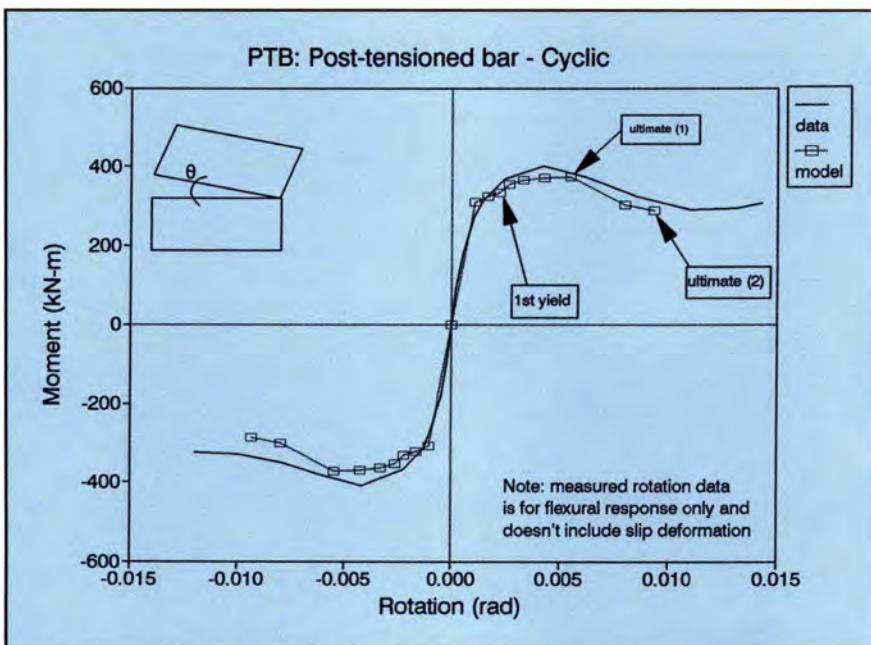


Fig. 16. Comparison of predicted vs. measured response.

0.63 and the flexural strength of the connection is 305 kN-m (224 kip-ft).

The plastic zone depth l_p can be determined using Eq. (4) as follows:

$$l_p = \frac{(1040 - 900)(15.875)}{(4)(3.0)} \\ = 185 \text{ mm (7.3 in.)}$$

Extension of the bar, δ_s , is determined from Eq. (3) as:

$$\delta_s = 2 \left[\frac{1}{2}(0.007 - 0.003)(397) + \right. \\ \left. (0.007 - 0.003)(185) + \right. \\ \left. \frac{1}{3}(0.035 - 0.007)(185) \right] \\ = 6.55 \text{ mm (0.26 in.)}$$

The rotation at ultimate state 2, θ_u , is evaluated using Eq. (1) as follows:

$$\theta_{u2} = \frac{6.55}{(1050 - 300)} = 0.0088$$

Other points of the moment-rotation response are determined using a computer spreadsheet following the same procedure described in the flowchart shown in Fig. 13. The complete predicted response is in good agreement with the measured flexural response excluding the slip deformation, as shown in Fig. 16 for Connection PTB.

CONCLUSIONS

The prestressed connections of precast wall panels investigated under cyclic loading behaved satisfactorily with sufficient ductility but with limited energy dissipation in comparison to mild steel connections. Based on the test results, the following conclusions can be drawn:

1. The behavior of the prestressed connection under cyclic loading conditions can be identified by three limit

states: (a) elastic stage prior to yielding; (b) nonlinear ductile stage without significant deterioration and with stable hysteresis; and (c) failure stage with significant deterioration.

2. The mode of failure for all the connections tested under cyclic loading was due to significant crushing and spalling of the drypack. In all configurations, except the unbonded connection, PTBU, the crushing at one end of the connection was accompanied by rupture of the reinforcement at the tension side.

3. All prestressed connections tested were able to withstand large inelastic deformations well beyond first yield with significant energy absorption capacity. A minimum ductility ratio of 6 was achieved by all types of connections.

4. Debonding of the prestressing continuity reinforcement across the connection more than doubled the deformation capacity, in comparison to the bonded connection, while slightly influencing the strength and stiffness.

5. At a given deformation level, the energy dissipation per cycle of the unbonded connection is lower than the bonded one. However, the cumulative energy dissipation for the unbonded connection at failure is higher due to significantly higher deformation capacity achieved by debonding.

6. The cyclic loading had a slight effect on the connection strength but significantly influenced the ductility of the connection. The ductility was reduced from 11 to 6 for connections prestressed with bars and from 7 to 6 for connections prestressed with strands.

7. Degradation of the stiffness was very sharp with the increase of the applied displacement. The residual stiffness was about 15 percent of the stiffness at yield.

8. The energy dissipation capacity of the prestressed connections was about one-half of that for the mild steel connections. The deformation capacity of prestressed connections was very similar to that of mild steel connections.

9. The proposed prediction procedure for the strength and drift capacity of prestressed connection configurations is in excellent agreement with the measured values.

DESIGN RECOMMENDATIONS

1. In general, prestressed connections for precast wall panels are characterized by sufficient ductility but limited energy dissipation in comparison to mild steel connections.

2. Prestressed bars appear to be a more suitable alternative than strands in connections for precast wall systems because they possess better energy dissipation characteristics with similar deformation capacity.

3. Debonding of prestressed reinforcement is a recommended detail to enhance the deformation capacity of the connection.

ACKNOWLEDGMENT

This experimental program was conducted at the University of Manitoba, Winnipeg, Manitoba, Canada, with financial assistance from the Natural Sciences and Engineering Research Council of Canada (NSERC), Con-Force Structures Ltd., and Super-Crete Ltd., Winnipeg, Manitoba, Canada. The assistance of graduate student Jeff West and laboratory technicians E. Lemke and M. McVey is greatly appreciated.

REFERENCES

1. *Uniform Building Code*, International Conference Building Officials, Whittier, CA, 1989.
2. SEAOC, *Recommended Lateral Force Requirements and Commentary*, Seismology Committee of the Structural Engineering Association of California, Sacramento, CA, 1990.
3. Soudki, K. A., "Behaviour of Horizontal Connections for Precast Concrete Loadbearing Shear Wall Panels Subjected to Large Reversed Cyclic Deformations," Ph.D. Thesis, University of Manitoba, Winnipeg, Manitoba, Canada, April 1994, 670 pp.
4. Soudki, K. A., Rizkalla S. H., and LeBlanc, B., "Horizontal Connections for Precast Concrete Shear Walls Under Cyclic Deformations — Part 1: Mild Steel Connections," *PCI JOURNAL*, V. 40, No. 4, July-August 1995, pp. 78-96.
5. ASTM, *Standard A 416 and Specification A 722*, American Society for Testing and Materials, Philadelphia, PA.
6. Llorente, C. A., "Inelastic Behaviour of Precast Shear Walls," Massachusetts Institute of Technology, Department of Civil Engineering, Research Report No. R81-25, Order No. 710, August 1981.
7. Bresler, B., and Pister, K. S., "Strength of Concrete Under Combined Stresses," *ACI Journal*, V. 55, No. 3, September 1958, pp. 321-345.
8. ACI Committee 318, "Building Code Requirements for Reinforced Concrete," American Concrete Institute, Detroit, MI, 1989.
9. French, C., Leon, R., and Grundhoffer, T., "Bond Behavior of Uncoated and Epoxy Coated Reinforcement in Concrete," Structural Engineering Report No. 92-04, Center of Transportation Studies, University of Minnesota, May 1992, 208 pp.
10. Pochanart, S., and Harmon, T., "Bond-Slip Model for Generalized Excitation Including Fatigue," *ACI Materials Journal*, V. 86, No. 5, 1989, pp. 465-474.
11. Paulay T., and Priestley, M., *Seismic Design of Reinforced Concrete and Masonry Buildings*, John Wiley & Sons, New York, NY, 1991.

APPENDIX — NOTATION

A_{ps} = area of prestressing reinforcement in tension	applied load	reinforcement at strain ϵ_{pe}
b = width of connection	δ_s = extension of prestressed reinforcement	f_{py} = yield stress in prestressing reinforcement at yield strain, ϵ_{py}
c = compression zone depth from extreme edge of connection subjected to compression	e = energy dissipation per cycle	f_{pu} = ultimate stress in prestressing reinforcement at ultimate strain, ϵ_{pu}
c' = length within compression zone, c , with ϵ_g less than ϵ_{gu}	E = cumulative energy dissipation	H = height of upper panel above connection region
d = distance from tension reinforcement to extreme edge of connection under compression	E_{ps} = Young's modulus of elasticity of prestressing steel	H_b = height of lugs of bar
d' = distance from compression reinforcement to extreme edge of connection under compression	ϵ_{gu} = ultimate compressive strain of drypack	K_y = stiffness at first yield
d_b = diameter of prestressing bar or strand	ϵ_{ps} = strain in prestressing reinforcement	K_u = stiffness at ultimate
Δ = displacement of top panel at location of applied load and relative to bottom panel	ϵ_{pe} = effective prestress strain in reinforcement after losses	l_e = elastic embedment length of tension reinforcement
Δ_r = flexural (rocking) deformation measured at top panel at location of applied load	ϵ_{py} = equivalent yield strain of prestressing reinforcement	l_p = plastic embedment length of tension reinforcement
Δ_s = slip deformation at connection region	ϵ_{pu} = ultimate tensile strain of prestressing reinforcement	S_b = clear space of lugs of bar
Δ_y = total displacement at first yield	f'_c = cylinder compressive strength of concrete at 28 days	μ_Δ = ductility ratio of Δ_u to Δ_y
Δ_u = total displacement at ultimate	f'_g = equivalent cylinder compressive strength of drypack at 28 days	θ = rotation of connection
Δf_s = stress increment in bar due to	f''_g = cube compressive strength of drypack grout	τ_g = shear stress within compression zone
	f_{ps} = stress in prestressing reinforcement at strain ϵ_{ps}	u_e = elastic bond strength of bar within elastic zone
	f_{pe} = effective stress in prestressing	u_f = frictional bond strength of bar within plastic zone
		x = length within compression zone, c , with ϵ_g greater than ϵ_{gu}